Conventional and microwave assisted hydrothermal syntheses of 11 Å tobermorite†
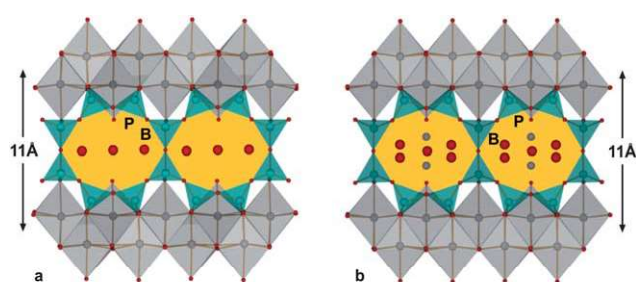
Sebastian Tränkle,[a] Denis Jahn,[b] Thomas Neumann,[c] Luc Nicoleau,[d] Nicola Hüsing[b] and Dirk Volkmer*[a]

The naturally occurring mineral 11 Å tobermorite is an important calcium silicate hydrate phase often used as a model structure for the poorly ordered calcium silicate hydrate phase (C-S-H) present in hydrated cement. In this work we present a hydrothermal synthesis of highly crystalline anomalous 11 Å tobermorite by conventional and microwave treatment. The microwave assisted synthesis provides a faster access to crystalline 11 Å tobermorite material in terms of reaction time, while the conventional method yields samples with a higher crystallinity. For conventional hydrothermal synthesis borosilicate glass was used as a Si precursor, which proves to be an excellent starting material for synthesis of highly crystalline 11 Å tobermorite. Furthermore, to the best of our knowledge, this is the first time the synthesis of unsubstituted 11 Å tobermorite by microwave synthesis is described. IR- and ^{29}Si-NMR spectroscopy reveals Q^3 Si–O tetrahedra sites only present in the double "dreierkette" structure typical for 11 Å tobermorite. The water content of the synthesized calcium silicate hydrates was examined by TGA which shows a weight loss (corrected for the loss of CO_2 from carbonate) of 8.3–10.7% for tobermorite samples from conventional synthesis and 10.6–12.5% for those from microwave assisted synthesis. While samples from microwave assisted synthesis typically showed a water loss from hydroxyl groups from DTG data at ∼760 °C, this could not be observed for tobermorite from conventional synthesis. By XRD investigations at different temperatures it could further be shown that the samples consist of the anomalous form of 11 Å tobermorite. The morphology of the needle-like tobermorite crystals was examined by AFM and HRTEM. The layered structure of 11 Å tobermorite could be visualized via the HRTEM investigations and the basal spacing of ∼11 Å could be measured directly.

Introduction

In the last decades the crystal structure of tobermorite, a naturally occurring calcium silicate hydrate mineral, was extensively investigated.[1–6] The structures of the forms of 11 Å tobermorite, namely normal and anomalous 11 Å tobermorite with the chemical formulae $Ca_5Si_6O_{17}(OH)_2 \cdot 5H_2O$ and $Ca_4Si_6O_{15}(OH)_2 \cdot 5H_2O$ respectively, are schematically shown in Fig. 1. These complicated structures, which have been solved using X-ray diffraction methods with natural tobermorite samples, occur in two main polytypes each, MDO_1 and MDO_2.[6] For anomalous 11 Å tobermorite these polytypes have been refined by Merlino et al. to $R = 0.128$ (MDO_1: orthorhombic, space group $F2dd$, $a = 11.265(2)$, $b = 7.386(1)$, $c = 44.970(9)$ Å) and $R = 0.051$ (MDO_2: monoclinic, space group $B11m$, $a = 6.735(2)$, $b = 7.385(1)$, $c = 22.487(4)$ Å, $\gamma = 123.25(1)°$).[6] While 11 Å represent the basal spacing between the characteristic layers of the structure, the terms "normal" and "anomalous" 11 Å tobermorite describe the thermal behavior of the two forms caused by different occupation of the interlayer spacing (highlighted in Fig. 1). While normal 11 Å tobermorite shrinks upon

[a]Chair of Solid State Chemistry, Institute of Physics, Universitätstrasse 1, 86159 Augsburg, Germany. E-mail: dirk.volkmer@physik.uni-augsburg.de

[b]Paris-Lodron University Salzburg, Hellbrunner Str. 34, A-5020 Salzburg, Austria

[c]SCHWENK Zement KG, 97753 Karlstadt, Germany

[d]BASF Construction Materials & Systems, BASF Construction Chemicals GmbH, 83308 Trostberg, Germany

Fig. 1 Scheme of the 11 Å tobermorite structure; (a) anomalous form, (b) normal form, turquoise: Si/Si–O tetrahedra, grey: Ca/Ca–O polyhedra, red: O; B: bridged Si–O tetrahedra, P: paired Si–O tetrahedra; hydrogen atoms are not shown.

heating in terms of the interlayer spacing due to reorganization of the Ca-cations in the spacing and the removal of water, anomalous 11 Å tobermorite maintains its basal spacing upon heating.

The interest in this mineral arises from its structural resemblance to the calcium silicate hydrate phases (C-S-H) in hydrated Portland cement.[2] In cement, these C-S-H phases often prove to be difficult to characterize by X-ray diffraction or electron microscopic methods due to their disordered nature. This disorder is mainly due to the small size of the coherent domains in the nanocrystalline material and the poor local order of the structure (*i.e.* short Si–O chains).[7] Accordingly the structure of C-S-H has not been resolved exactly to date. Therefore, studying the parameters influencing the crystallinity and size of tobermorite crystals may help to further elucidate the structure or the source of disorder of poorly ordered C-S-H phases.

Hydrothermal syntheses of crystalline 11 Å tobermorite material have been reported by several research groups so far, with reaction times ranging from a few hours to a couple of months using different Si precursors.[8–15] While the crystallinity of samples in older publications is often described as "very high" in terms of having 25 or more peaks in XRD patterns,[8,9] more recent publications commonly include XRD data exhibiting the most common peaks of the tobermorite structure with reasonable crystallinity.[13–15]

Microwave synthesis approaches often have the advantage of accelerating the reaction time in comparison to conventional hydrothermal syntheses.[16–18] Querol *et al.* reported on a comparison of the recycling of fly-ash by hydrothermal and microwave treatment, which resulted in a mixture of zeolites and other silicates, among others also including tobermorite. The reaction time found for the microwave treatment compared to the conventional hydrothermal treatment was 50 to 100 times faster.[16] Tae *et al.* reported the hydrothermal treatment of blast furnace slag also partly resulting in the formation of tobermorite. In this study, the reaction time found for the microwave treatment was 16 times faster than that found for the conventional hydrothermal treatment.[17] Miyake *et al.* synthesized Al-substituted tobermorite from calcium oxide, aluminum hydroxide, colloidal silica and sodium hydroxide by conventional and microwave hydrothermal reactions. XRD measurements showed that while both synthesis routes resulted in the same product, microwave treatment yielded a faster reaction time.[18]

The aim of the present work was to develop a synthetic approach giving access to 11 Å tobermorite of high crystallinity, which is preferable for electron microscopy investigations, with a reasonable reaction time. We therefore report on the synthesis of highly crystalline 11 Å tobermorite by hydrothermal synthesis *via* a customized oven and by microwave treatment. The influence of the choice of silicon precursors on the product was investigated by carrying out the synthesis with different precursors, namely quartz, silicic acid and borosilicate glass. The latter one proved to be an excellent precursor for this type of synthesis. Furthermore different quartz precursors with defined particle sizes have been evaluated for microwave synthesis.

The crystalline material was characterized with respect to its structure and chemical composition by X-ray diffraction (XRD), high resolution transmission electron microscopy (HRTEM), atomic force microscopy (AFM), infrared spectroscopy (IR), ^{29}Si magic angle spinning nuclear magnetic resonance spectroscopy (^{29}Si MAS-NMR) and thermogravimetric analysis (TGA).

Experimental

According to a synthesis protocol described by Huang *et al.* which yielded a highly crystalline tobermorite phase,[15] the starting materials in the present work were chosen as follows: $Ca(OH)_2$, ethylenediamine tetraacetic acid (EDTA) as a chelating agent and a Si source. Using only amorphous SiO_2 did not result in crystalline tobermorite material in our experiments. According to El-Hemaly *et al.* amorphous silica as a silicon precursor shows a rather slow reaction concerning the formation of tobermorite due to two possible reasons: (a) a too high concentration of dissolved silicon in the reaction mixture or (b) a fast reaction into C-S-H phases that do not transform into tobermorite under hydrothermal conditions.[8]

We therefore followed a different approach by using silicon sources, which dissolve slower than amorphous SiO_2 under hydrothermal conditions, such as borosilicate glass and quartz.

Materials

For a typical hydrothermal synthesis, 0.356 g (4.8 mmol) of reagent grade $Ca(OH)_2$ (p.a. Merck) and a defined amount of Si precursor (borosilicate glass (Pyrex glass), quartz (SiO_2) and/or silicic acid (Sigma Aldrich $SiO_2 \cdot H_2O$, <20 μm), see Table 1) in the desired Ca to Si molar ratio (Ca/Si ratio) were added to 120 mL of demineralized water in a 200 mL teflon-lined Berghof steel autoclave.

Table 1 Starting materials and reaction parameters of hydrothermally synthesized samples

Ca/Si_0	Si precursor	Reaction time (days)	EDTA[a]	Sample
0.36	Borosilicate glass (11 mmol Si) + silicic acid (2.4 mmol)	7	X	b-1
0.36	Borosilicate glass (11 mmol Si) + silicic acid (2.4 mmol)	7	—	b-2
0.36	Borosilicate glass (13.4 mmol Si)	7	—	b-3
0.44	Borosilicate glass (10.7 mmol Si)	7	—	b-4
0.60	Borosilicate glass (8.1 mmol Si)	7	—	b-5
0.89	Borosilicate glass (5.4 mmol Si)	7	—	b-6
1.78	Borosilicate glass (2.7 mmol Si)	7	—	b-7
0.44	Quartz glass (10.8 mmol)	7	—	q-1
0.36	Silicic acid (13.4 mmol)	7	—	s-1

[a] X: addition of 0.048 mmol EDTA; —: no addition of EDTA.

The exact amount and type of precursor added, the starting Ca/Si ratio (Ca/Si_0) used, and the reaction parameters are summarized in Table 1. For synthesis with addition of EDTA 0.048 mmol of EDTA (p.a. Merck) was added to the reaction mixture. As the starting Ca/Si ratio does not necessarily represent the Ca/Si ratio in the product, ratios ranging from 0.36–1.78 have been tested. The pH of the reaction mixture was adjusted to 13 by adding 4 M KOH.

The steel autoclave was placed in a special rotating mount inside the oven and rotated at 200 °C for 7 days. After this time the autoclave was cooled down to room temperature. The product was thoroughly washed with demineralized water and afterwards dried in a desiccator under vacuum.

To investigate the influence of the main elemental constituents (Si, B, Na, Al and Fe) of the borosilicate glass employed in the formation of tobermorite, a series of syntheses was carried out using silicic acid (Sigma-Aldrich, <20 μm) and the oxide compounds of different elements as precursors in the proportions present in the borosilicate glass. The type of glass (Pyrex glass) being used usually consists of the following main components by weight: ~81% SiO_2, ~13% B_2O_3, ~4% Na_2O, ~2% Al_2O_3 and ~0.04% Fe_2O_3.

The microwave synthesis was performed with a Berghof 'speed-wave four' microwave with custom firmware in order to achieve a reaction time exceeding 2 h. For synthesis 0.148 g (2 mmol) of reagent grade $Ca(OH)_2$ (p.a. Merck) was added to 50 mL of demineralized water in the 90 mL teflon-lined Berghof DAK-100 vessel. The pH was adjusted to 13 with the addition of 4 M KOH before adding 0.067 g (1 mmol) of silicic acid (Sigma-Aldrich, <20 μm) and a certain amount of an additional Si source (borosilicate glass, quartz of different particle sizes, silicic acid) depending on the desired Ca/Si ratio. The vessel was then treated by microwave irradiation for 8 h at 200 °C. The amount and type of precursor added, the Ca/Si ratio employed and the reaction parameters are summarized in Table 2. After cooling to room temperature the product was washed with demineralized water and dried in a desiccator under vacuum.

Characterization

TEM investigations were performed using a JEOL 2100F microscope with a FEG electron source operated at 200 kV. The microscope is equipped with a Gatan image filter (GIF). For sample preparation, a small portion of material was dispersed in ethanol and sonicated for 5 minutes. Holey carbon-coated copper grids were then dipped into the dispersion and dried at RT.

Atomic force microscopy (AFM) measurements were carried out with an Agilent 5500 scanning probe microscope under ambient conditions. The data were collected *via* contact or tapping mode in closed loop configuration with a large multipurpose closed-loop scanner. Olympus silicon cantilevers TR800PSA (pyramidal tip, typical spring constant 0.15 N m^{-1}, typical tip-radius 20 nm) and Nanosensors FM cantilevers (pyramidal tip, typical spring constant 2.8 N m^{-1}, typical resonance frequency ~75 kHz, typical radius <10 nm) were used for contact mode and tapping mode measurements respectively. The tobermorite crystals were scanned at a speed of 0.3–0.5 lines per

Table 2 Starting materials and reaction parameters of microwave synthesized samples

Ca/Si_0	Si precursor	Reaction time (h)	Sample
0.36	Quartz (<0.063 mm; 4.50 mmol) + silicic acid (1 mmol)	8	q-1-MW
0.45	Quartz (<0.063 mm; 3.44 mmol) + silicic acid (1 mmol)	8	q-2-MW
0.60	Quartz (<0.063 mm; 2.33 mmol) + silicic acid (1 mmol)	8	q-3-MW
0.70	Quartz (<0.063 mm; 1.86 mmol) + silicic acid (1 mmol)	8	q-4-MW
0.83	Quartz (<0.063 mm; 1.41 mmol) + silicic acid (1 mmol)	8	q-5-MW
0.36	Borosilicate glass (4.50 mmol Si) + silicic acid (1 mmol)	8	b-1-MW
0.36	Borosilicate glass (4.50 mmol Si) + silicic acid (1 mmol)	12	b-2-MW
0.36	Silicic acid (5.60 mmol)	8	s-1-MW

second. To ensure that the crystals were bound on the sample holder while scanning in contact mode, the tobermorite needles were glued to an AFM disc *via* a special resin using the following procedure adapted from Yang *et al.*[19] The samples were dispersed in demineralized water and then sonicated for 5 minutes. One drop of the dispersion was transferred to an AFM disc coated with a resin (TEMPFIX) at approximately 40 °C and dried at RT. Opensource SPM data analysis software 'Gwyddion' has been used for handling the topography data and extraction of profiles.[20]

X-ray diffraction patterns were recorded using a Panalytical X'Pert Pro MPD (conventional hydrothermal synthesis) or a Seiffert XRD 3003 TT system (microwave assisted synthesis) equipped with a GE Meteor 1D detector. All measurements were performed in Bragg–Brentano geometry using Cu Kα1 radiation.

Infrared spectra of the samples were recorded using a Bruker Equinox 55 equipped with a Bruker Platinum ATR unit from 4000–400 cm^{-1} using 4 cm^{-1} resolution and 32 scans per sample.

Solid-state NMR experiments were carried out using a Bruker Avance 400 at a ^{29}Si resonance frequency of 79.5 MHz and a spinning rate of 11 kHz.

The resulting Ca/Si molar ratio in the samples was measured by inductively coupled plasma optical emission spectrometry (ICP-OES) using a Varian Vista MPX radial. To dissolve the samples for ICP-OES measurements 0.100 g of C-S-H material was molten with 1.80 g $LiBO_2$ in a platinum crucible at 1000 °C and dissolved in 100 mL 5% v/v HCl. The solution was then diluted to 200 mL with demineralized water while using 10 mL of Y_2O_3 as an internal standard according to the procedure described by Farinas *et al.* for cementitious samples.[21] According

to Farinas *et al.* the high amount of HCl and LiBO$_2$ in the samples leads to strong matrix effects which were corrected by measuring calibration curves with a reference material dissolved using the procedure described above. This reference material was prepared by mixing known amounts of SiO$_2$ (quartz, Fluka) and Ca(OH)$_2$ (p.a. Merck) resulting in a Ca/Si ratio of 0.8.

Thermogravimetric analysis (TGA) was performed using a TA Instruments Q500 with 5 K min^{-1} heating rate under nitrogen flow in the temperature range from r.t. up to 1000 °C (sample weight 10–15 mg).

Results and discussion

The main objective of this work is to investigate the effect of the silicon source, the reaction time and the starting Ca/Si ratio on the formation of a crystalline tobermorite phase. The conventional hydrothermal synthesis was carried out with and without EDTA to investigate the influence of the chelating effect and thus slower release of calcium on the synthesis as described by Huang *et al.*[15] Furthermore, a protocol for the microwave assisted synthesis route was developed and directly compared to the conventional hydrothermal route. In hydrothermal synthesis microwave treatment often has advantages over conventional heat treatment (*i.e.* samples kept in an oven under hydrothermal conditions) in terms of reaction time.[22] In the case of Al-substituted tobermorite Miyake *et al.* reported microwave assisted synthesis with a short reaction time.[18] In our experiments the use of the microwave assisted route also showed a faster reaction time for synthesizing a pure, unsubstituted (no partial substitution of Si by Al or other elements in the structure) 11 Å tobermorite phase.

Furthermore, to the best of our knowledge, this is the first report of a microwave assisted synthesis of unsubstituted 11 Å tobermorite.

Structure

The conventional hydrothermal synthesis has been performed using different Si precursors, namely borosilicate glass, quartz and silicic acid. Fig. 2a shows the corresponding XRD patterns. The highest crystallinity (measured by means of width and intensity of the reflections in the XRD patterns, amorphous material in the product shown with AFM/TEM and existence of Q^3 sites in IR and ^{29}Si-NMR data) could be achieved by using borosilicate glass as the silicon precursor, however, all precursors were suited to produce crystalline 11 Å tobermorite. All samples of this series show a sharp peak at ~8 °2theta representing the 002 spacing of 11 Å between the individual 'dreierkette' chains in tobermorite. All synthesized tobermorite phases show close resemblance to the structure of anomalous 11 Å tobermorite found by Merlino *et al.*[6] The use of borosilicate glass with a Ca/Si$_0$ of 0.36 (Fig. 2a, sample b-3) results in minor formation of a gyrolite-like structure, another C-S-H mineral, indicated by weak reflections at 21 and 50 °2theta.

Tobermorites typically change their crystal structure upon heating. Normal 11 Å tobermorite (Ca$_5$Si$_6$O$_{17}$(OH)$_2$·5H$_2$O; Ca/Si = 0.83) transforms to 9 Å tobermorite upon heating to ~300 °C, caused by the rearrangement of the zeolitic Ca
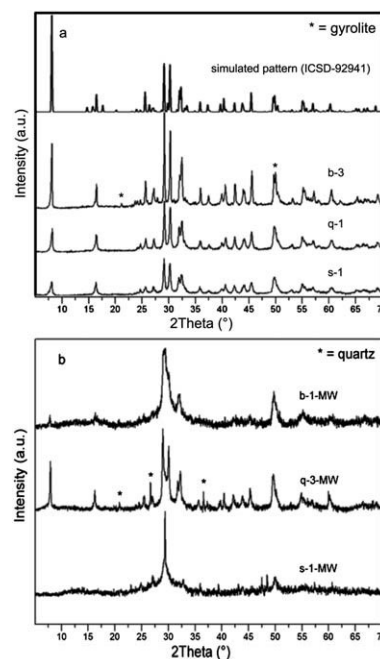
Fig. 2 XRD patterns of samples from different Si precursors (borosilicate glass, quartz, silicic acid), (a) simulated pattern (anomalous 11 Å tobermorite, structure determined by Merlino *et al.*[6]) and conventional hydrothermal synthesis; (b) microwave assisted synthesis.

ions in the interlayer spacing.[6,23] Anomalous tobermorite (Ca$_4$Si$_6$O$_{15}$(OH)$_2$·5H$_2$O; Ca/Si = 0.67) does not contain zeolitic Ca ions in the interlayer spacing and therefore does not transform to 9 Å tobermorite upon heating. This could also be verified for our samples by *in situ* X-ray diffraction using a heating chamber. No shift of the basal reflection at d = 11 Å upon heating to 400 °C could be observed (see Fig. A in the ESI†).

The influence of the different components of borosilicate glass on the synthesis of crystalline tobermorite was examined by addition of B$_2$O$_3$, Na$_2$O, Al$_2$O$_3$, SiO$_2$ and Fe$_2$O$_3$ to the starting mixture according to the composition of the glass. There was no evidence found for B$_2$O$_3$, Na$_2$O, Al$_2$O$_3$ or Fe$_2$O$_3$ to induce the formation of highly crystalline tobermorite. The presence of the basal reflection at ~8 °2theta indicating the formation of tobermorite layers could only be observed for samples with additional SiO$_2$ (lower Ca/Si ratio). XRD patterns of the series are given in Fig. B in the ESI.†

For the purpose of comparison and to investigate whether the reaction time can be decreased, microwave assisted syntheses were also carried out using the three different Si precursors. Fig. 2b shows XRD patterns of the resulting products. While all products from microwave assisted synthesis exhibit inferior crystallinity compared to products from conventional synthesis, the best results regarding the crystallinity of the synthesized phase could be achieved by using quartz in combination with silicic acid as the Si precursor. The use of silicic acid as the sole silicon source did not give the desired crystalline product, but a mostly amorphous C-S-H phase without long-range order which did not show a reflection representing a basal spacing in X-ray diffraction measurements.

The use of borosilicate glass resulted in tobermorite, but the crystallinity is lower compared to the use of quartz. The short reaction time of 8 h did not allow the whole borosilicate glass to be dissolved in the reaction mixture, therefore undissolved pieces of borosilicate glass could still be found in the vessel after synthesis.

For the short reaction time small amounts of amorphous silica seem to be necessary to get an intermediate C-S-H phase of low crystallinity, which then reacts with quartz (or borosilicate glass) to yield crystalline tobermorite.[9] Small amounts of unreacted quartz are still present in the product.

Fig. 3 shows the XRD patterns of hydrothermally synthesized samples using borosilicate glass as the Si precursor with the Ca to Si ratio ranging from 0.36 to 1.78. Sample b-1 was prepared with the addition of EDTA and showed no advantage with respect to its crystallinity over samples without the addition of EDTA (b-2). The addition of silicic acid to the starting mixture also had no influence on the resulting product (b-3). Samples b-1 to b-3 show minor formation of gyrolite-like structures.

The Ca/Si ratio could be raised to 0.60 (Fig. 3a, sample b-5) without losing the tobermorite structure or producing other calcium silicate hydrate phases in significant amounts. For a Ca/Si ratio of 0.89 (Fig. 3b, sample b-6) xonotlite, another layered calcium silicate hydrate, was formed in addition to tobermorite. Xonotlite is a common product in the hydrothermal synthesis of C-S-H phases occurring at temperatures above 160 °C.[24]

For a Ca/Si ratio of 1.78 (Fig. 3b, sample b-7) a mixture of calcium silicates and calcium silicate hydrates (mainly larnite: Ca_2SiO_4) was observed. The reaction time for the hydrothermal
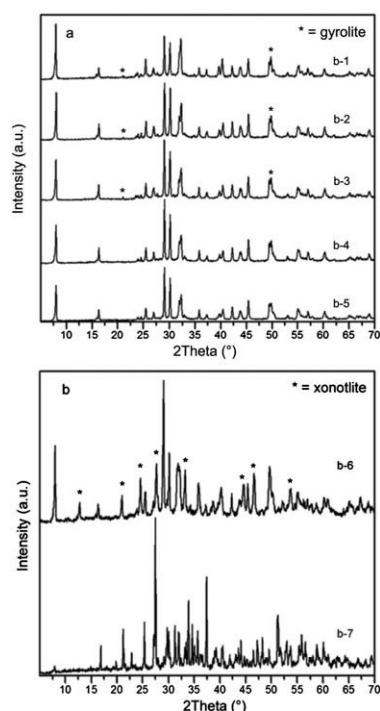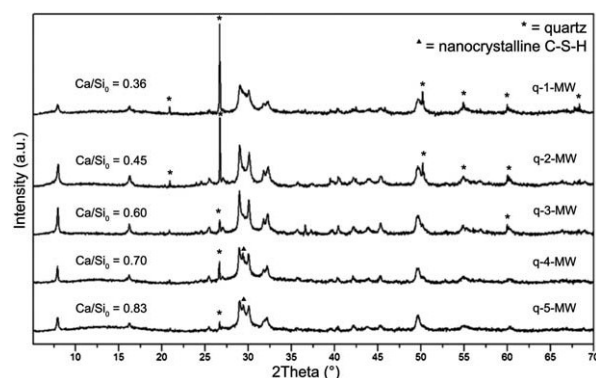

Fig. 4 XRD patterns of samples from microwave assisted synthesis with the Ca to Si ratio ranging from 0.36–0.83.

synthesis using borosilicate glass was also evaluated from 1 to 7 days. Formation of crystalline 11 Å tobermorite could be observed with a reaction time ≥1 day, while complete dissolution of the Si precursors occurred with a reaction time ≥2 days. The maximum yield of tobermorite was achieved with a reaction time ≥3 days. For the microwave assisted synthesis, the best results regarding the phase purity and crystallinity were achieved upon using quartz (Fluka, <0.063 μm) with addition of silicic acid as silicon source and using a Ca to Si ratio of the starting materials of 0.60. Fig. 4 shows XRD patterns of microwave synthesized samples with the Ca/Si ratio ranging from 0.36 to 0.83. While it was possible to synthesize 11 Å tobermorite from all those Ca/Si ratios, using ratios below 0.60 resulted in high amounts of unreacted quartz in the product. With a starting Ca/Si ratio higher than 0.60 the product was less crystalline and showed reflections at ~29.3 °2theta ($d = \sim 3.05$ Å) suggesting the formation of nanocrystalline C-S-H.[18,25]

In addition to the XRD data presented above the determination of the Ca/Si ratio by ICP-OES also provides insight into the structure of the samples. The results for highly crystalline 11 Å tobermorite from conventional synthesis (b-1; Ca/Si = 0.63) and microwave assisted synthesis (q-3-MW; Ca/Si = 0.74) are shown in Table 3. Taking into account the structure found by Merlino *et al.* for anomalous 11 Å tobermorite ($Ca_4(Si_6O_{15})(OH)_2(H_2O)_5$; equates to Ca/Si = 0.67), the sample from hydrothermal synthesis has a slightly lower ratio.[6] For the sample from microwave assisted synthesis the observed Ca/Si ratio is slightly higher than the theoretical value of the anomalous 11 Å tobermorite structure. Deviations of the resulting Ca/Si ratio from the theoretical value probably arise from defects in the structure of the crystalline material. The influence of structural variation on the Ca/Si ratio of calcium silicate hydrates has been discussed in detail by Richardson.[26] Hence,

Fig. 3 XRD patterns of samples from conventional hydrothermal synthesis with the Ca to Si ratio ranging from 0.36–1.78.

Table 3 Results of ICP-OES investigations

| Sample	Ca [mg L^{-1}]	Si [mg L^{-1}]	Ca/Si (molar)
b-1	112.3	124.2	0.63
q-3-MW	124.5	118.6	0.74
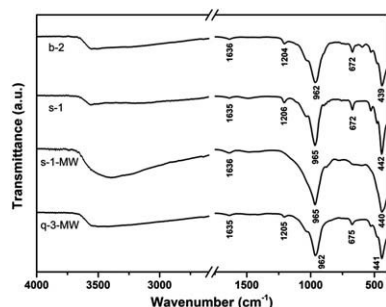
Fig. 5 IR spectra of samples from conventional and microwave assisted synthesis; range between 4000 and 2600 cm^{-1} magnified; b-2: conventional synthesis with borosilicate glass, Ca/Si$_0$ = 0.36; s-1: conventional synthesis with silicic acid, Ca/Si$_0$ = 0.36; s-1-MW: microwave synthesis with silicic acid, Ca/Si$_0$ = 0.36; q-3-MW: microwave synthesis with quartz and silicic acid, Ca/Si$_0$ = 0.60.

higher values could be explained by a varying degree of protonation of the silanol groups in the tobermorite structure: lower degrees of protonation result in higher Ca/Si ratios, as the charges of deprotonated silanol groups are mostly compensated by Ca^{2+} ions.[26] On the other hand higher degrees of protonation result in lower Ca/Si ratios. The omission of bridging Si-O tetrahedra in the structure (compare with Fig. 1) or the incorporation of additional Ca^{2+} ions balanced by additional OH$^-$ ions also results in a higher Ca/Si ratio.[26]

The IR-spectra recorded of samples from conventional and microwave assisted synthesis shown in Fig. 5 exhibit the typical bands for crystalline 11 Å tobermorite material.[23,27] The band at ~440 cm^{-1} can be assigned to deformation of the Si-O tetrahedra, as well as the band at ~480 cm^{-1}. The band at around 670 cm^{-1} is due to Si-O-Si bending vibrations of the Si-O tetrahedra. The stretching vibrations of Q^2 sites are represented by the intense band at ~960 cm^{-1} and the shoulder at ~1060 cm^{-1}. These sites correspond to the Si-O tetrahedra chains found in the tobermorite structure (Fig. 6).

All samples that were identified as highly crystalline 11 Å tobermorite by X-ray diffraction show a band at around 1200 cm^{-1}, which correlates with the Q^3 silicon sites specific for 11 Å tobermorite.[27] These sites are due to the bridging 'dreierkette' Si-O tetrahedron, which is surrounded by three Si-O tetrahedra (Fig. 6). For the sample synthesized with silicic acid in the microwave, this band is not present, which is probably due to the low crystallinity of the sample. The band at ~1630 cm^{-1} is
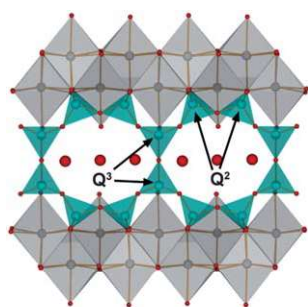
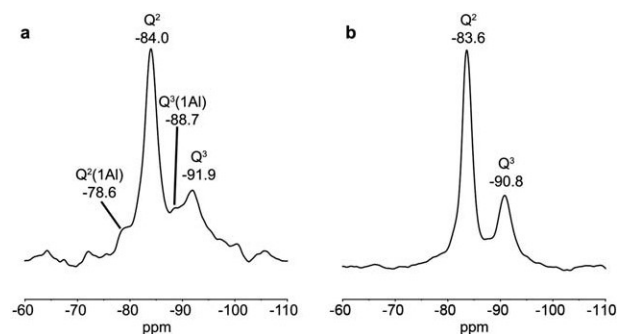due to the H-O-H bending vibrations. In the region of ~3000 to 3600 cm^{-1} the spectra all show a very broad band corresponding to O-H stretching vibrations.

By means of ^{29}Si-NMR (SP MAS) investigations it is possible to detect whether the use of different silicon sources affects the connectivity of the Si-centers of the synthesized sample by identifying different Q sites correlating with the linkage of the Si-O tetrahedra.

Several Q sites could be identified as a function of the used silicon source (borosilicate glass and quartz respectively). In both cases Q^2 and Q^3 signals (see Fig. 7) could be observed, though there were slight deviations in comparison to results found in the literature. Maeshima *et al.* presented ^{29}Si-NMR data for naturally occurring 11 Å tobermorite with signals for the Q^2 sites (chain groups) located at around -83.8 to -85.3 ppm and signals for Q^3 sites (chain branching) at -96.1 ppm.[28] Further detailed investigations were performed concerning the incorporation of heteroatoms such as aluminum from the borosilicate glass compared to samples prepared from quartz (aluminum free) as the silicon source. Maeshima *et al.* also showed Q^2(1Al) and Q^3(1Al) sites in the range of -80.5 ppm to -91.9 ppm.[28] As shown in Fig. 7 we have measured a signal for Q^3 at -91.9 ppm (synthesis with borosilicate glass) and -90.8 ppm (synthesis with quartz glass), respectively. Our Q^3(1Al) and Q^2(1Al) signals in Fig. 7a were located at -88.7 ppm and -78.6 ppm, respectively. The shift into lower field is typical for Al substituted tobermorite. The sample shown in Fig. 7b was synthesized without an Al source (only quartz glass), so Q^3(1Al) signals are not observed. Taking this into consideration the signal at -90.8 ppm can only be assigned to Q^3. Maeshima *et al.* are referring to Wieker *et al.* who also found Q^2 and Q^3 sites for 11 Å tobermorite located at -85 to -89 ppm and -95 to -100 ppm, respectively.[24] As shown with IR investigations, all of our hydrothermally synthesized tobermorite samples exhibit Q^3 sites, which is in good agreement with the ^{29}Si-NMR (SP MAS) results. This also correlates with the high crystallinity of the samples observed *via* XRD measurements and the associated high order of the structure which leads to the formation of Q^3 sites.

In order to check the influence of the drying conditions of the samples on the bulk weight loss during thermogravimetric analysis, four different methods were tested after synthesis and drying as described in the experimental section (drying in a desiccator under vacuum) for one sample (q-3-MW). The TGA

Fig. 6 Schematic structure of anomalous 11 Å tobermorite showing Q^2- and Q^3-sites in the silicate chain.

Fig. 7 ^{29}Si-NMR spectra of hydrothermally synthesized samples with borosilicate glass and quartz; (a) b-2; (b) q-1.

has been performed after synthesis and standard drying without further treatment, directly after stirring a small amount of the sample in dry ethanol followed by washing under suction with dry acetone, after storage at 11% rh over a saturated LiCl solution for 3 days and after storage of the sample at 60 °C under nitrogen for 3 days adapted from ref. 25. The resulting four TGA plots (see ESI†) show similar behavior concerning the weight loss from ~130 °C up to 1000 °C and only minor differences in the loss of adsorbed water on the sample surface (weight loss up to ~94 °C). This loss was minimized when drying the sample at 60 °C under nitrogen for 3 days, thus all samples were dried prior to TGA using this method.
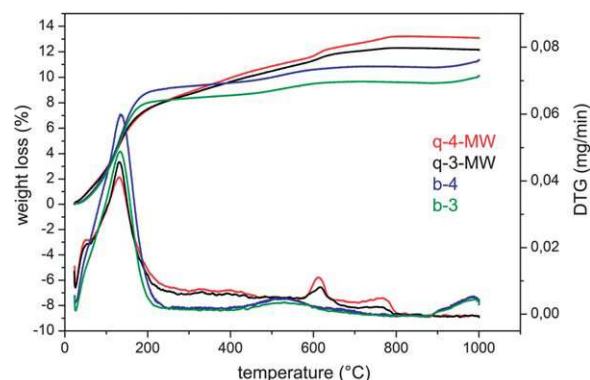
TGA of the synthesized samples containing tobermorite shows a bulk weight loss in the range of 7.3–13.3%, which is mainly due to the loss of water. Small amounts of $CaCO_3$ are present in most of the samples, which is due to carbonation when exposed to air. Therefore, decomposition of $CaCO_3$ can be observed during TGA through the weight loss due to release of CO_2 at around 600 °C.[25] The resulting corrected weight loss was calculated for the synthesized samples. A summary of the TGA data for all samples is given in Table 4. The TGA and DTG plots of four selected samples from microwave and conventional hydrothermal synthesis are shown in Fig. 8. The traces show typical behavior for tobermorite material, with a major weight loss up to ~200 °C, gradual weight loss between 200 and 400 °C and minor weight loss between 400 and 800 °C.

The corrected weight loss gives information about the water content of the samples and is in the typical range for tobermorite material. Shaw et al. determined a (uncorrected) bulk weight loss of 12.2% for naturally occurring anomalous 11 Å tobermorite, which is close to the values determined with our measurements, which in turn are well below the weight loss for nanocrystalline calcium silicate hydrate phases (~20% depending on the Ca/Si ratio).[29,30]

Fig. 8 TGA and DTG plots of selected samples from conventional and microwave assisted synthesis.

For samples from microwave assisted synthesis the bulk/corrected weight loss was higher than for samples from conventional synthesis, which is probably due to formation of nanocrystalline C-S-H phases (also observed through TEM and XRD investigations) and the lower overall crystallinity. As mentioned earlier nanocrystalline phases exhibit higher water content and therefore raise the overall weight loss of the samples.[29,30] Lower crystallinity should result in a higher number of hydroxyl groups in the structure, which in turn would also increase the bulk weight loss of the samples through hydroxyl condensation in the temperature range of 730–830 °C.[30] This can also be observed for our microwave samples through the DTG signal at ~760 °C in Fig. 8.

Sample b-6 exhibits a significantly lower weight loss compared to the other samples from conventional synthesis, which should be due to formation of xonotlite also observed in XRD measurements. The bulk weight loss of natural xonotlite was determined by Shaw et al. to be 2.5%, which represents the loss of water from structural hydroxyl groups at around 800 °C.[29] Therefore the bulk/corrected weight loss of sample b-6, which represents a mixture of tobermorite and xonotlite (see XRD data in Fig. 3b), lies in between the bulk weight loss of tobermorite and xonotlite. For sample b-7 the bulk weight loss was 7.3%. As the sample is a mixture of different calcium silicates and calcium silicate hydrates (compare XRD data in Fig. 3b) this value is not significant. The bulk weight loss of sample s-1-MW (19.5%) is also not significant, as the sample contained no tobermorite phase according to XRD data.

Table 4 Results from TGA

Bulk weight loss (%)	Corrected weight loss (%)	Starting Ca/Si	Sample
10.8	9.2	0.36	b-1
10.8	9.9	0.36	b-2
10.1	9.2	0.36	b-3
11.4	10.4	0.44	b-4
11.6	10.7	0.60	b-5
7.7	6.7	0.89	b-6
7.3	—[a]	1.78	b-7
10.0	9.0	0.44	q-1
10.5	8.3	0.36	s-1
11.6	11.3	0.36	q-1-MW
11.0	10.5	0.44	q-2-MW
12.1	11.3	0.60	q-3-MW
13.1	12.1	0.70	q-4-MW
13.3	12.5	0.83	q-5-MW
12.1	11.5	0.36	b-1-MW
13.7	11.5	0.36	b-2-MW
19.5	—[a]	0.36	s-1-MW

[a] Corrected weight loss not determined (b-7: hydroxylated larnite shows the loss of OH at ~650 °C,[29] the loss of CO_2 from carbonate overlaps with this temperature range; s-1-MW: overlapping DTG signals around 600 °C).
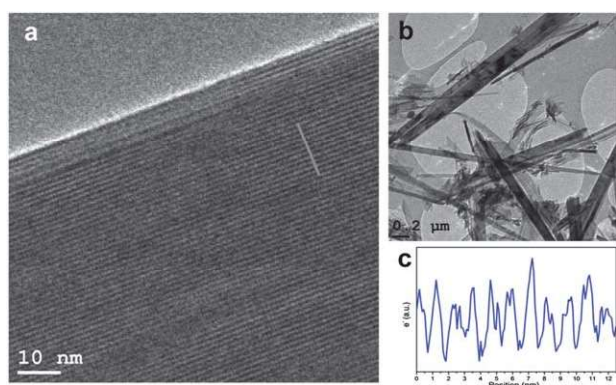
Morphology

The morphology of the synthesized samples has been investigated by HRTEM and AFM measurements. Tobermorite crystallizes in plate-like form or fibers depending on the Ca/Si ratio, the temperature and the pH used for hydrothermal reaction.[15,31] We observed fiber-like crystals under the conditions used in our experiments (starting pH of 13/200 °C), which is consistent with the results of Huang et al.[15]

Fig. 9a and 10a show the layer-like structure of the crystals constituted of 'dreierkette' Si–O-tetrahedra chains and the Ca–O backbone with sixfold coordinated Ca. With the help of TEM
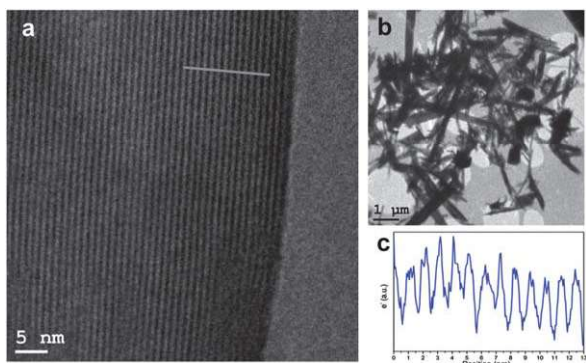
Fig. 9 (a and b) TEM images of tobermorite from hydrothermal synthesis; (c) profile extracted from the area as shown by the white line in (a); sample: b-1.
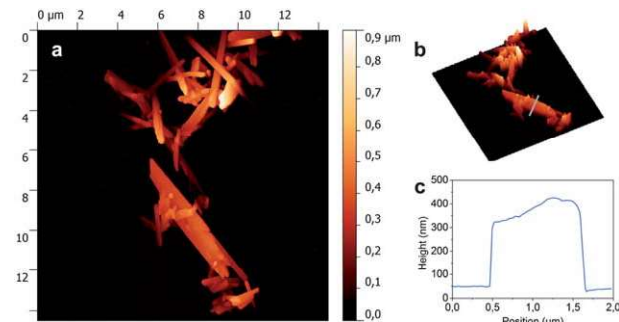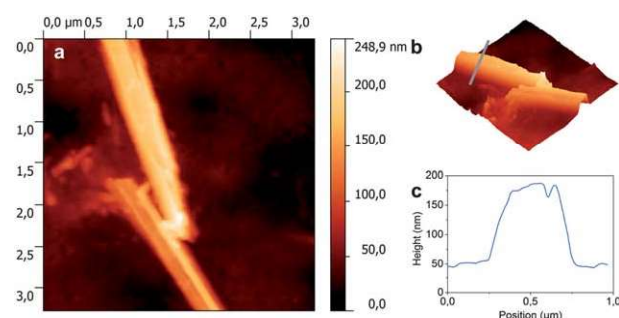

Fig. 11 (a) Topographical AFM image of hydrothermally synthesized tobermorite; (b) the corresponding 3D projection; (c) height-profile of needle-like crystal in (b); sample: b-1.

Fig. 10 (a and b) TEM images of tobermorite from microwave assisted hydrothermal synthesis; (c): extracted profile from (a); sample: q-3-MW.

correlates with the XRD investigations showing a lower overall crystallinity of the samples and featured reflections indicating nanocrystalline C-S-H.

The aim of the AFM measurements was to visualize steps on the surface of the crystals and the topography of the crystals itself, in order to draw a conclusion on the number of layers which assemble the crystal.

The topographical AFM images show tobermorite needles from conventional and microwave assisted synthesis (Fig. 11 and 12). The size of the needles corresponds to those found in the TEM investigations. The use of AFM for morphological investigations also provides insights into the thickness of the needles by extracting profiles from the topographical data (Fig. 11c and 12c). For tobermorite obtained by conventional synthesis the length and thickness were ~7.6 μm and ~370 nm respectively, although it is not clearly visible from the topographical images whether or not the needle is comprised of one, or layers of more than one particle. For the needle-like crystal synthesized by the microwave assisted method shown in Fig. 12 the length and thickness were ~3.9 μm and ~130 nm respectively, which is, despite the undefined constitution of the particles, significantly smaller than the size of needles from conventional hydrothermal synthesis. An image of the whole crystal used for thickness and length measurements is included in the ESI.†

AFM measurements of the samples synthesized by the microwave assisted route confirm the results of XRD and TEM investigations concerning the crystallinity of the material which

investigations it is possible to visualize the 002 spacing of 11 Å tobermorite directly and measure it by extracting electron density profiles from the images (Fig. 9c and 10c). The extracted profile shows a 002 spacing of ~11.2 Å for the sample of conventionally synthesized tobermorite and a mean basal spacing of the layers measured over the 9 layers shown in the profile of ~11.6 Å for microwave assisted synthesis. While the measurement of the 002 spacings from TEM images is dependent on the orientation of the sample on the sample-holder, the obtained values are in good agreement with the spacings derived from XRD data.

The possibility to visualize the layers of the structure by TEM investigations arises from the high crystallinity of the samples also observed by XRD. Fig. 9b and 10b show the needle-like tobermorite crystals from conventional and microwave assisted synthesis, respectively. The size of these needles varied from smaller than 1 μm to ~10 μm.

While the TEM investigations exhibit the needle-like morphology of the tobermorites for both synthesis routes, the samples obtained by microwave assisted synthesis also showed material with crumpled-foil morphology, which can typically be observed for nanocrystalline C-S-H phases.[26,32] Microwave assisted synthesis of Al-substituted tobermorite from zeolites also shows this morphology in SEM investigations.[33] This

Fig. 12 (a) Topographical AFM image of microwave synthesized tobermorite; (b) the corresponding 3D projection; (c) height-profile of needle-like crystal in (b); sample: q-3-MW.

is composed of the needle-like tobermorite crystals and (X-ray) amorphous particles surrounding these crystals.

The number of layers which assemble the crystal could not directly be calculated from the AFM data. The problem arises from the random orientation of the crystals on the sample-holder, therefore it was not possible to determine in which direction the layers of the crystals are stacked.

Conclusions

Not only a hydrothermal route towards highly crystalline anomalous 11 Å tobermorite has been developed in this work, but also a new approach based on the microwave assisted synthesis is presented. In both cases, the crystallinity is highly dependent on the choice of silicon precursor, the used Ca/Si ratio as well as the reaction time.

The best results regarding the crystallinity and phase-purity of the samples in hydrothermal synthesis could be achieved by using borosilicate glass as the Si precursor with a Ca to Si ratio between 0.44 and 0.60. Other Si precursors or higher Ca/Si ratios resulted in formation of undesired C-S-H phases.

Microwave assisted synthesis showed the best results regarding the crystallinity and phase-purity by using a mixture of quartz and small amounts of silicic acid as the Si precursor with a Ca/Si ratio of 0.60. Small amounts of unreacted quartz are still present in the product. Furthermore TGA revealed a weight loss for samples from microwave assisted synthesis at ~760 °C. This loss might be due to release of water from hydroxyl groups, which indicates lower crystallinity compared to samples from conventional synthesis or the presence of nanocrystalline C-S-H also observed by TEM and AFM measurements.

We could show that microwave synthesis shortens the reaction time for hydrothermal synthesis of 11 Å tobermorite (from 7 days with conventional synthesis to 8 h using the microwave assisted route), though best results regarding the crystallinity are achieved by the conventional method. When using boro-silicate glass as Si precursor the use of microwave assisted synthesis is limited due to the slow dissolution process at high pH of the starting material. The reaction time of 8 h is not sufficient for complete dissolution of glass material. We believe that this process in the conventional hydrothermal synthesis is the key to prepare a highly crystalline tobermorite phase. To verify this thesis we conducted a series of hydrothermal syntheses using precursors in a proportion, which resembled the composition of the borosilicate glass. It could be shown that none of the additional elements (other than Si) play a signifi-cant role in the formation of a highly crystalline tobermorite phase.

On the other hand it is possible to synthesize tobermorite *via* the microwave route and the use of quartz with small amounts of silicic acid in a relatively short reaction time. As described above the crystallinity for microwave synthesized tobermorite is not as high as that for conventionally produced material.

By the suitable choice of the synthesis route, Ca to Si ratio and Si precursors it is therefore possible to tailor the tober-morite material in terms of crystallinity and reaction time as favored or needed for further experiments.

Notes and references

1 S. A. Hamid, *Z. Kristallogr.*, 1981, **154**, 189.
2 I. G. Richardson, *Cem. Concr. Res.*, 2008, **38**, 137.
3 H. D. Megaw and C. H. Kelsey, *Nature*, 1956, **177**, 390.
4 S. Merlino, E. Bonaccorsi and T. Armbruster, *Am. Mineral.*, 1999, **84**, 1613.
5 S. Merlino, E. Bonaccorsi and T. Armbruster, *Eur. J. Mineral.*, 2000, **12**, 411.
6 S. Merlino, E. Bonaccorsi and T. Armbruster, *Eur. J. Mineral.*, 2001, **13**, 577.
7 A. Nonat, *Cem. Concr. Res.*, 2004, **34**, 1521.
8 S. El-Hemaly, T. Mitsuda and H. Taylor, *Cem. Concr. Res.*, 1977, **7**, 429.
9 C. F. Chan and T. Mitsuda, *Cem. Concr. Res.*, 1978, **8**, 135.
10 D. S. Snell, *J. Am. Ceram. Soc.*, 1975, **58**, 292.
11 N. Hara, C. Chan and T. Mitsuda, *Cem. Concr. Res.*, 1978, **8**, 113.
12 A. Winkler and W. Wieker, *Z. Anorg. Allg. Chem.*, 1979, **451**, 45.
13 R. Houston, R. S. Maxwell and S. A. Carroll, *Geochem. Trans.*, 2009, **10**, 1.
14 J. Kikuma, M. Tsunashima, T. Ishikawa, S. Matsuno, A. Ogawa, K. Matsui and M. Sato, *IOP Conf. Ser.: Mater. Sci. Eng.*, 2011, **18**, 022017.
15 X. Huang, D. Jiang and S. Tan, *J. Eur. Ceram. Soc.*, 2003, **23**, 123.
16 X. Querol, A. Alastuey, A. López-Soler, F. Plana, J. M. Andrés, R. Juan, *et al.*, *Environ. Sci. Technol.*, 1997, **31**, 2527.
17 S.-J. Tae, T. Tanaka and K. Morita, *ISIJ Int.*, 2009, **49**, 1259.
18 M. Miyake, S. Niiya and M. Matsuda, *J. Mater. Res.*, 2011, **15**, 850.
19 T. Yang, L. Holzer, R. Kagi, F. Winnefeld and B. Keller, *Ultramicroscopy*, 2007, **107**, 1068.
20 D. Nečas and P. Klapetek, *Cent. Eur. J. Phys.*, 2012, **10**, 181.
21 J. C. Farinas and P. Ortega, *Analusis*, 1992, **20**, 221.
22 N. Kuhnert, *Angew. Chem.*, 2002, **114**, 1943.
23 T. Mitsuda and H. Taylor, *Mineral. Mag.*, 1978, **42**, 229.
24 W. Wieker, A.-R. Grimmer, A. Winkler, M. Mägi, M. Tarmak and E. Lippmaa, *Cem. Concr. Res.*, 1982, **12**, 333.
25 K. Garbev, G. Beuchle, M. Bornefeld, L. Black and P. Stemmermann, *J. Am. Ceram. Soc.*, 2008, **91**, 3005.
26 I. G. Richardson, *Cem. Concr. Res.*, 2004, **34**, 1733.
27 P. Yu, R. J. Kirkpatrick, B. Poe, P. F. McMillan and X. Cong, *J. Am. Ceram. Soc.*, 1999, **82**, 742.
28 T. Maeshima, H. Noma, M. Sakiyama and T. Mitsuda, *Cem. Concr. Res.*, 2003, **33**, 1515.
29 S. Shaw, C. Henderson and B. Komanschek, *Chem. Geol.*, 2000, **167**, 141.
30 G. Renaudin, J. Russias, F. Leroux, F. Frizon and C. Cau-dit-Coumes, *J. Solid State Chem.*, 2009, **182**, 3312.
31 G. L. Kalousek and A. F. Prebus, *J. Am. Ceram. Soc.*, 1958, **41**, 124.
32 S. Komarneni, E. Breval, D. M. Roy and R. Roy, *Cem. Concr. Res.*, 1986, **16**, 580.
33 S. Komarneni, J. S. Komarneni, B. Newalkar and S. Stout, *Mater. Res. Bull.*, 2002, **37**, 1025.